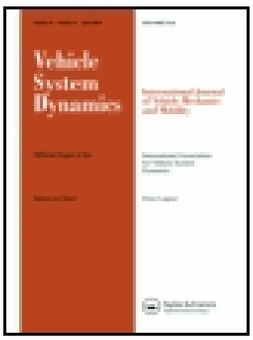

Taylor & Francis
Taylor & Francis Group

Vehicle System Dynamics
International Journal of Vehicle Mechanics and Mobility

ISSN: (Print) (Online) Journal homepage: https://www.tandfonline.com/loi/nvsd20

# A signal analysis based hunting instability detection methodology for high-speed railway vehicles

Jianfeng Sun , Enrico Meli , Wubin Cai , Hongxin Gao , Maoru Chi , Andrea Rindi & Shulin Liang

**To cite this article:** Jianfeng Sun , Enrico Meli , Wubin Cai , Hongxin Gao , Maoru Chi , Andrea Rindi & Shulin Liang (2020): A signal analysis based hunting instability detection methodology for high-speed railway vehicles, Vehicle System Dynamics, DOI: 10.1080/00423114.2020.1763407

**To link to this article:** https://doi.org/10.1080/00423114.2020.1763407

Published online: 07 Jun 2020.

VEHICLE SYSTEM DYNAMICS
https://doi.org/10.1080/00423114.2020.1763407



# A signal analysis based hunting instability detection methodology for high-speed railway vehicles

Jianfeng Sun [a], Enrico Meli[b], Wubin Cai[a], Hongxin Gao[a], Maoru Chi [a], Andrea Rindi[b] and Shulin Liang[a]

[a]State Key Laboratory of Traction Power, Southwest Jiaotong University, Chengdu, People's Republic of China; [b]Department of Industrial Engineering, Florence University, Italy

**ABSTRACT**

Hunting stability is a long-standing research topic and has been deeply investigated due to its great influence on railway vehicle dynamic performances. Most of the existing hunting monitoring methods detect only the large amplitude hunting instability (LAHI). However, the small amplitude hunting instability (SAHI) is still hard to be detected accurately and efficiently. To face this challenging problem, this paper describes a signal analysis based hunting instability detection methodology. The proposed method is based on cross-correlation techniques and is able to detect both SAHI and LAHI in a simple, efficient and effective way. Eight cross-correlation indicators (CCIs) are exploited to detect anomalous SAHI and LAHI conditions. A fully detailed dynamic model of one typical high-speed railway vehicle is developed to test the methodology and to compare the CCIs under different vehicle operating conditions. The most effective CCI and its critical values are determined on the basis of the statistics and comparisons of the simulation results. Furthermore, the robustness of the proposed method to distinguish hunting instability and periodic excitations coming from track irregularities has been verified. Finally, the proposed instability detection methodology has been validated by detecting the SAHI successfully on field test data coming from specific experimental campaigns.

**ARTICLE HISTORY**
Received 14 January 2020
Revised 3 April 2020
Accepted 25 April 2020

**KEYWORDS**
High-speed railway vehicles; small amplitude hunting instability; fault detection; cross-correlation analysis

## 1. Introduction

The rapid increase in the operating mileage of high-speed railway and in the operation speed make the safety and security technologies of high-speed railway face enormous challenges. In this framework, the hunting motion, characterised by self-excited lateral-yaw oscillations, is one of the key aspects in vehicle system dynamics and has been deeply studied throughout the development of railway vehicles [1,2]. The hunting motion occurs at a certain speed called the critical speed, which determines the actual operating speed of the railway vehicle. Once the vehicle speed exceeds the critical speed, the vibration amplitude increases with increasing speed and eventually causes a violent lateral swing of the wheelset, which deteriorates the ride comfort, makes the vehicle prone to derailment, damages the

**CONTACT** Shulin Liang a_slliang@163.com

track and induces fatigue failure in vehicle structure. Therefore, it is of great importance to develop accurate hunting instability detection methods, not only for vehicle design purposes but also for safety reasons under operating conditions. To face this problem, in this work a signal analysis based hunting instability detection method for high-speed railway vehicles is proposed. More particularly, the proposed strategy is based on cross-correlation techniques and is able to detect in a simple, efficient and effective way both small and large amplitude hunting instabilities. The proposed detection method has been validated by means of field test data coming from specific experimental campaigns performed by the authors' research group.

There are different evaluation parameters for the lateral stability assessment on high-speed railway vehicles in existing standards. A moving Root Mean Square (RMS) of the sum of guiding forces, the sum of lateral axle box forces and lateral accelerations on bogie frame above axle boxes can all be used to assess the stability of the vehicle [3–8].

The guiding forces and lateral axle box forces are the most effective parameters to assess the vehicle running stability, as they can well highlight the influence of bogie hunting motion on the vehicle running safety. However, both these forces need instrumented wheelset to be measured and the instrumented wheelsets need to be recalibrated frequently, which is highly expensive and not suitable for standard activities [9]. The bogie lateral accelerations are generally adopted for the hunting instability detection around the world. In China, as the operating speed has increased up to 350 km/h, all the 'Renaissance' high-speed trains are equipped with accelerometers on bogie frame above axle boxes for hunting stability monitoring. Based on the bogie lateral acceleration, there exist two kinds of methods in the standards for the hunting instability assessment. The first one is to adopt the RMS of the acceleration as the evaluation value, and the instability frequency has to be determined before the evaluation of test results [4]. The second one is to identify the number of times when the peak value of the acceleration exceeds the limit value continuously [8]. However, the definitions of stability in mechanics and in railway practice are usually not identical. Consequently, the results of stability assessment through these two methods are different from that by the way of a bifurcation calculation, especially in the case of the supercritical bifurcation [10–12]. Figure 1 shows the time-domain signals and the assessment results of the two methods based on the bogie frame lateral acceleration. It can be seen that the methods mentioned above can detect the large amplitude hunting instability (LAHI: amplitude of lateral acceleration signals from bogie frame exceed the safety limit), but cannot detect the small amplitude hunting instability (SAHI: amplitude of lateral acceleration signals from bogie frame is within the safety limit, but the wheel has a small displacement perturbation). At the same time, further problems may arise due to delays or early withdrawals of the alarm in existing monitoring systems.

Concerning SAHI detection, many researchers have conducted specific studies on this problem. Wang et al. [13] introduced the basic concept of vibration energy method to judge the bogie hunting instability of freight wagon. As the frequency range to consider is different, this method is not suitable for high-speed vehicles. Yao et al. [14] applied the RMS of bogie lateral acceleration under different frequency band as a criterion to evaluate the lateral stability of high-speed trains by considering the most unfavourable track conditions and by improving the safety margin. Numerical simulation shows that the proposed method can lead to early warning for bogie slight hunting instability, but that some key parameters have to be tuned in advance on the basis of a large number of

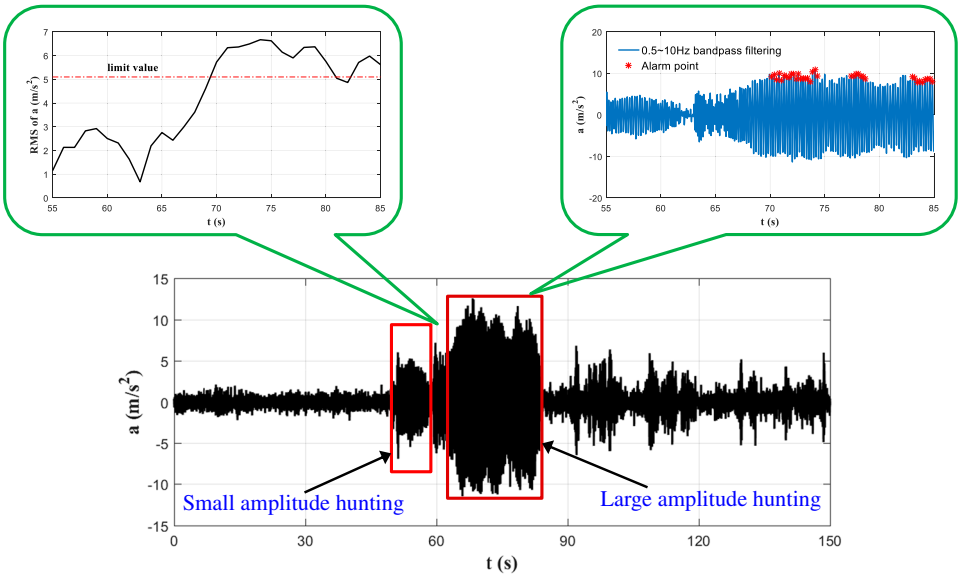


**Figure 1.** Time-domain signals and the assessment results for the two methods based on the bogie frame lateral acceleration.

test data. Gasparetto et al. [15] proposed a method to monitor the running stability in a high-speed railway bogie by using the random decrement technique and Prony method. Numerical experiments and line tests showed the capability of the method to separate the case of a bogie with new wheel profiles from a condition with worm profiles. Based on Multiscale Permutation Entropy and Local Tangent Space Alignment, Ning et al. [16] proposed a feature extraction method to distinguish the different states of complex signals and to identify the bifurcation evolution of small amplitude hunting signals. Empirical mode decomposition (EMD) is a common approach to decompose and extract local characteristic signals, especially for the analysis and processing of nonlinear nonstationary signals [17]. To address the issue of SAHI for high-speed train, a new method [18,19] which combines ensemble empirical mode decomposition (EEMD), entropy features and least squares support vector machine (LSSVM) was proposed to diagnose hunting abnormal motion state. To improve the robustness of the small-amplitude hunting monitoring methods, Ye et al. [20] proposed an idea of the bogie frame's lateral-longitudinal-vertical data fusion and a new feature extraction method. The field test results showed that this method is superior to the single lateral diagnosis method. Based on the vibration signals of axle box, the indirect monitoring method for wheelset lateral displacement was proposed for bogie hunting instability detection in [21]. The amplitude of wheelset lateral motion corresponding to hunting instability can be calculated by the singular value decomposition through Hankel matrix. The degree of hunting instability thus can be evaluated by focusing on the displacement amplitude.

In the real-time monitoring system, not only the identification accuracy but also the computational efficiency and robustness of an algorithm are really important. However, the calculation accuracy and efficiency of identification algorithm are often conflicting requirements, especially for signal decomposition methods [16–21]. Furthermore, the robustness

of the algorithm is often not concerned enough and only the bogie acceleration is taken into account in the above methods.

Actually, there exist strong correlation between the bogie and the carbody vibration during the hunting instability, and this correlation can be effectively exploited to detect hunting instability [22]. Cross-correlation analysis is a widely used method in the railway industry for health monitoring of railway vehicle suspension system. Mei [23,24] established a method of fault detection and condition monitoring for the primary suspension of railway vehicles based on signal cross-correlation analysis. This method is very sensitive to different fault conditions. Li [25,26] developed a fully detailed dynamic model of 40t axle load heavy haul wagon. With the help of auto-correlation and cross-correlation analysis, the fault diagnosis for secondary bolster spring was studied, and an online fault diagnosis strategy was proposed.

The work described in this paper starts from some ideas described in [23–26] concerning the application of cross-correlation techniques to detect suspensions faults in railway vehicles and making use of measurement coming from axle-box, bogie and carbody, and tries to extend and apply such ideas to a new field, the detection of the hunting instability.

More particularly, faults in suspensions usually cause an imbalance in vehicle dynamic systems, resulting in dynamic interferences between different vibrations, which provides a key indication to distinguish between normal and abnormal states of suspensions. Similarly, once the vehicle hunting instability occurs, the vibration characteristics of the vehicle system in different directions and the vibration transmission among different components change significantly. On the basis of this characteristics change, this work attempts to diagnose the hunting instability for high-speed vehicles from the perspective of cross-correlation analysis between different acceleration signals coming from bogie and carbody. The goal of the proposed detection method is to identify both the LAHI and the SAHI effectively. In this way, if the cross-correlation analysis shows hunting instability, the driver can take effective measures such as lowering the speed timely to prevent the train from reaching LAHI.

This paper is organised as follows. In Section 2, the mathematical introduction of cross-correlation analysis is presented and the proposed detection method for hunting instability is introduced. In Section 3, a fully detailed dynamic model of one typical high-speed railway vehicle is developed for numerical simulations. Some cross-correlation indicators (CCIs) are proposed to describe the cross-correlation of the considered signals and are compared to each other under different vehicle operating conditions. In this way, the most effective CCI and its critical value in detecting hunting instabilities is determined on the basis of the obtained results and of the comparisons. In Section 4, robustness analysis of the proposed method is carried out to distinguish the hunting instability and the periodic excitations from the track irregularities. In Section 5, the proposed detection method is validated by means of field test data coming from specific experimental campaigns performed by the authors' research group.

## 2. Hunting instability identification via cross-correlation analysis

The signal-based hunting instability detection method for high-speed railway vehicles is developed in this section. The new method relies on the cross-correlation analysis of the

sensor-collected acceleration signals measured on bogie and carbody. The method aims at detecting the incipient instability of the bogie in advance, before the level of bogie vibration can trigger an alarm due to the conventional instability detectors.

## 2.1. Cross-correlation analysis

The correlation analysis methods for vibration signals mainly rely on the concepts of correlation function and correlation coefficient to study the correlation and the mutual dependence between two signals. The cross-correlation coefficient has been widely used in the signal processing field to explore the similarity of two signals or determine the positions of vibration source via the time lag [27–29].

Here, the definition of cross-correlation coefficient is briefly introduced and illustrated from a mathematical point of view. By way of example two different time-series signals $x(t)$ and $y(t)$ are considered. Equation (1) gives the cross-correlation coefficient between these two signals at time lag of $\tau$:

$$\delta_{xy}(\tau) = \frac{R_{xy}(\tau) - \mu_x \mu_y}{\sigma_x \sigma_y} \tag{1}$$

where $\mu_x$ and $\mu_y$ are the mean values of the signals, $\sigma_x$ and $\sigma_y$ are the standard deviations of the signals, and $R_{xy}(\tau)$ is the cross-correlation function associated to the two signals. For discrete random signals, $R_{xy}(\tau)$ can be expressed as follows:

$$R_{xy}(\tau) = \frac{1}{N}\left(\sum_{n=1}^{N-|\tau|} x_n y_{n+\tau}\right), \quad \tau = 0, \pm 1, \pm 2, \ldots \tag{2}$$

where $N$ is the sample number considered for the signals couple. The cross-correlation coefficient is a number between $-1$ and 1.

The cross-correlation curves show the cross-correlation coefficient $\delta_{xy}(\tau)$ between two signals on a certain range of time lag $\tau$. In Figure 2(a,b), by way of example, the cross-correlation analyses of acceleration random and purely harmonic signals are carried out to highlight the difference in the cross-correlation behaviour. The signals window is equal to 10 s. Signal A1 and signal A2 are white noise while signal B1 and signal B2 are sine waves (same periods and different phases) added with white noise. It can be seen that the cross-correlation curve between signal A1 and signal A2 is nearly zero until the time lag $\tau$ is close to the signal window (in such condition the correlation analysis is useless). The cross-correlation curve between signal B1 and B2 is harmonic with increasing time lag $\tau$. The amplitude of the cross-correlation curves reaches 1, and the period of the curves is the same of the original signals. Obviously, there exists a significant difference in the cross-correlation curves between random signals and harmonic signals with the same period. This difference can be effectively exploited for the hunting instability detection.

## 2.2. Methodology

The proposed detection methodology is shown in Figure 3. In the first step, the vehicle geometric and kinematic parameters and the track characteristics are inserted as inputs into

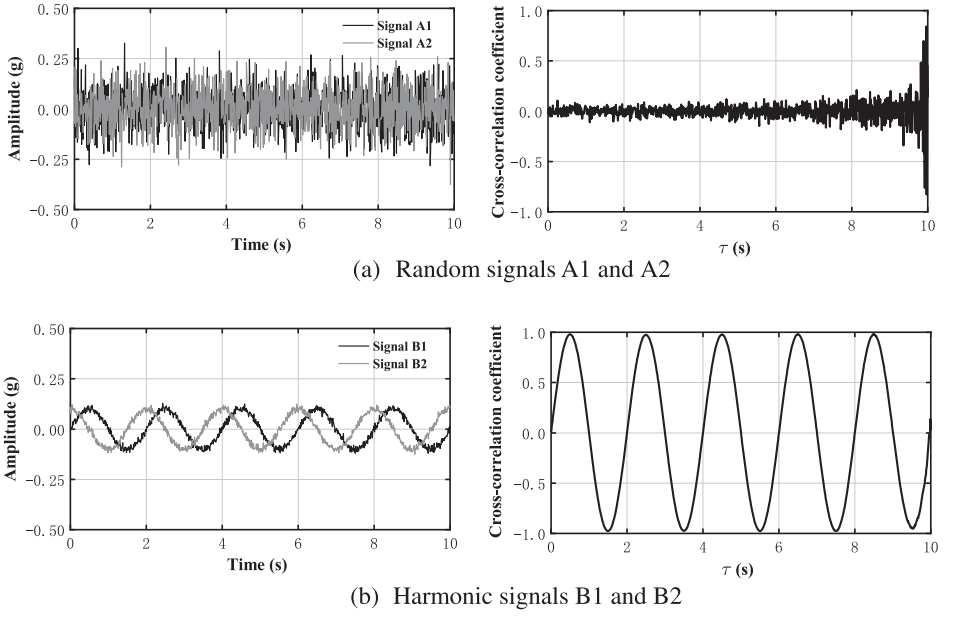


**Figure 2.** The time history of the signals $x(t)$ and $y(t)$ and cross-correlation curves for (a) random signals and (b) harmonic signals.

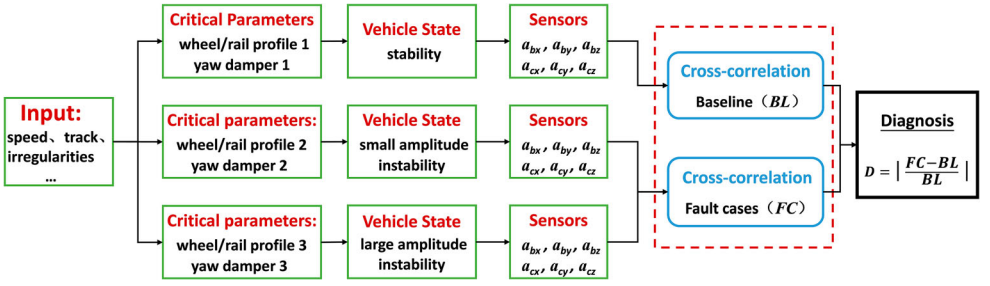


**Figure 3.** Flowchart of the proposed hunting instability detection methodology.

the high-speed railway vehicle dynamic model. The wheel/rail profiles and yaw damper characteristics are two critical parameters for the critical speed and bifurcation type of the vehicle. In the second step, three kinds of vehicle states (including stability, SAHI and LAHI) are reproduced by adjusting the critical parameters. The acceleration signals of bogie frame and carbody are collected in three directions ($x$, $y$, $z$) by the simulated sensors simultaneously.

The simulated sensors are installed both on the carbody and on the bogie frame; the sensors locations are illustrated in Figure 4. The sensor $A\_b1$ is located at the rear-right part of the rear bogie and acquires the longitudinal, lateral and vertical acceleration signals ($A\_b1\_X$, $A\_b1\_Y$ and $A\_b1\_Z$). The sensor $A\_b2$ is located in the middle of the rear bogie and acquires the lateral acceleration signal ($A\_b2\_Y$). The sensor $A\_b3$ is located at the front-left part of the front bogie, and acquires the lateral acceleration signal ($A\_b3\_Y$). Two sensors $A\_c1$ and $A\_c2$ are mounted on the rear-right and front-left parts of the carbody

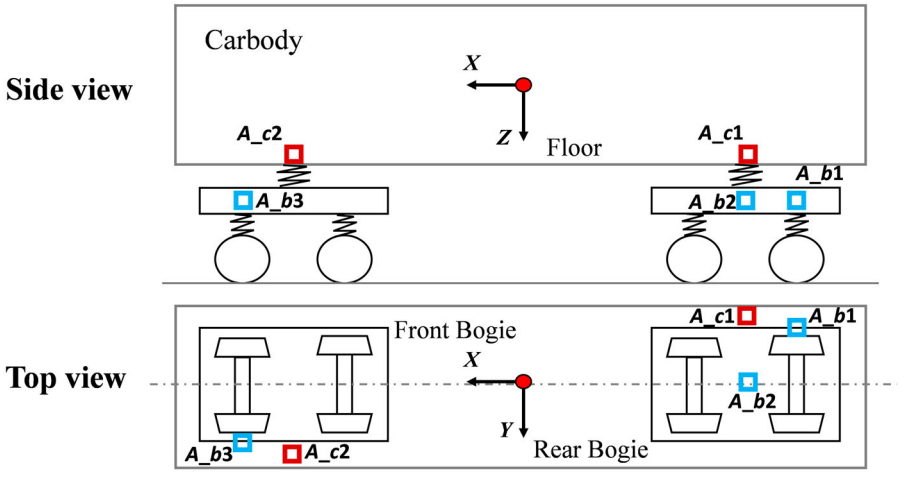


**Figure 4.** Sensor arrangement on the railway vehicle model.

floor. The sensor $A\_c1$ acquires the longitudinal, lateral and vertical acceleration signals ($A\_c1\_X$, $A\_c1\_Y$ and $A\_c1\_Z$) while the sensor $A\_c2$ acquires the lateral acceleration signal ($A\_c2\_Y$).

The cross-correlations between the sensor-collected acceleration signals are calculated and analysed to extract various dynamic behaviours of the bogie frame and carbody in proposed vehicle states. The cross-correlation analyses focused on in this paper include three categories:

- Category 01: cross-correlation between the acceleration signals coming from the bogie frame.
- Category 02: cross-correlation between the acceleration signals coming from the carbody.
- Category 03: cross-correlation between the acceleration signals coming from the bogie frame and carbody.

Among the cross-correlations included in Category 01, 02 and 03, eight cross-correlation indicators are proposed in this paper as CCIs (see Table 1). Taking the cross-correlation indicator $B\_XY$ as an example, the character $B$ denotes the bogie frame (while the character $C$ denotes the carbody) and the characters $XY$ denote the directions of acceleration signals used to calculate the cross-correlation. In particular, $B\_Y\varphi$ denotes the cross-correlation between the lateral acceleration and yaw angle acceleration of the bogie frame. The yaw angle acceleration can be easily derived from lateral accelerations of $A\_b1$ and $A\_b2$ and from the knowledge of the carbody wheel base.

The phase delay between the bogie and carbody acceleration signals may exist on account of the suspension system transmission characteristic [22]. As a result, the cross-correlation at 0.0 s time shift doesn't reach the peak value. The cross-correlation analysis introduced above show that the amplitude of cross-correlation curve in one period can distinguish the random signal and harmonic signal effectively. As the hunting frequency is basically larger than 1 Hz [22], the maximum of cross-correlation coefficient between the

**Table 1.** Cross-correlation indicators (CCIs).

| Category | CCI | Description | Acceleration signals |
|---|---|---|---|
| Category 01 | *B_XY* | Cross-correlation between the acceleration signals from the bogie frame | *A_b1_X*, *A_b1_Y* |
| | *B_YZ* | | *A_b1_Y*, *A_b1_Z* |
| | *B_Yφ* | | *A_b1_Y*, *A_b2_Y* |
| | *B_YY* | | *A_b1_Y*, *A_b3_Y* |
| Category 02 | *C_XY* | Cross-correlation between the acceleration signals from the carbody | *A_c1_X*, *A_c1_Y* |
| | *C_YZ* | | *A_c1_Y*, *A_c1_Z* |
| | *C_YY* | | *A_c1_Y*, *A_c2_Y* |
| Category 03 | *BC_YY* | Cross-correlation between the acceleration signals from the bogie frame and carbody | *A_b1_Y*, *A_c1_Y* |

time shift of 0.0 and 1.0 s would be an appropriate indicator, and is therefore used in this paper to evaluate the cross-correlation between acceleration signals.

The inputs of the third step are the CCIs previously described, that is the acceleration cross-correlations calculated for the three different vehicle states. The CCIs for the stability case are considered as baseline (BL) (for example, *B_XY*_BL) whereas the CCIs of the SAHI and LAHI cases are considered as fault cases (FC) (for example, *B_XY*_SAHI and *B_XY*_LAHI). For each CCI, the relative diagnosis indicator *D* can be calculated as well, like for instance:

$$\begin{cases} D = |(B\_XY\_SAHI - B\_XY\_BL)/B\_XY\_BL| \, for \, SAHI \\ D = |(B\_XY\_LAHI - B\_XY\_BL)/B\_XY\_BL| \, for \, LAHI \end{cases} \tag{3}$$

At this point, the fault diagnosis is finally performed by properly comparing the CCIs and their statistical parameters under different vehicle states (stability, SAHI and LAHI conditions), see Section 3. The strategy proposed to reach this goal is very efficient and tries to minimise the number of unknown parameters that have to be set up and tuned a priori.

## 3. Application of the proposed methodology to simulated scenarios

In order to numerically test the proposed procedure, a suitable multibody model of railway vehicle has been developed and numerical simulations have been carried out to study the behaviour of the eight CCIs under different vehicle states (stability, SAHI and LAHI conditions). Starting from these simulations, the most effective CCIs and their critical values have been determined to detect the hunting instability of the high-speed vehicles, especially for SAHI.

### 3.1. Recurrence of different vehicle states

To calculate the CCIs described in the previous section, the required vehicle states (stability, SAHI and LAHI conditions) have to be reproduced through suitable multibody simulations, and the acceleration signals mentioned in Table 1 have to be collected simultaneously.

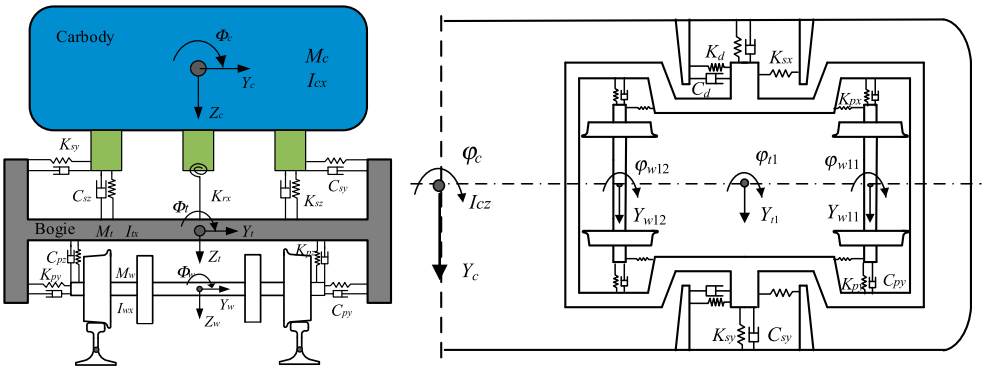


**Figure 5.** Multibody model of the railway vehicle.

To reach this goal, a complete railway vehicle multibody model has been developed in SIMPACK. The vehicle model is considered as a rigid multibody system composed of 4 conventional wheelsets, 8 axle boxes, two pairs of bogie frame, one carbody, primary and suspensions, as shown in Figure 5. The carbody and the bogie frames are characterised by six independent degrees of freedom (DoFs) which allow free movements and rotations with respect to the longitudinal, lateral and vertical directions, respectively. Concerning the wheelsets, six DoFs are considered, but only four DoFs are independent and two of them ($z$-axis, rotation about $x$-axis) are dependent. Finally, the axle boxes are characterised with one DoF with respect to the wheelset (rotation about $y$-axis). Overall, 42 independent DoFs are considered for rigid motions in this model. The vehicle in the model runs with constant speed on the straight line. The primary vehicle parameters used in the simulation are listed in Appendix.

To reproduce various vehicle states (stability and, especially SAHI and LAHI conditions), the nonlinearities of wheel/rail contact and yaw damper have to be carefully taken into account. Considering the standard rail profile CHN60, three kinds of wheel profile are used in the simulation, and the related equivalent conicity are calculated starting from the wheel/rail contact geometry and according to the standard regulation in force UIC 519 [30], as shown in Figure 6(a,b) respectively. Wheel profile 1 is the standard profile S1002CN whereas wheel profile 2 as well as wheel profile 3 are measured worn profiles. The match of wheel/rail profile 2 shows a decreasing equivalent conicity function in the range of amplitudes between 0 and 3 mm. The wheelsets thus possess a large gravity stiffness at a small amplitude which limits the further increase of the wheelset lateral displacement, leading to supercritical bifurcation with low limit cycles. On the contrary, the match of wheel/rail profile 3 shows an increasing equivalent conicity function in the range of amplitudes between 0 and 3 mm. Consequently, once the running speed exceeds the nonlinear critical speed, the vehicle dynamics shows a subcritical bifurcation characterised by a sudden transition from stable behaviour to a pronounced limit cycle [31]. In general, the linear critical speed corresponding to wheel/rail profile 3 is larger than that corresponding to wheel/rail profile 2, as its equivalent conicity is smaller.

Figure 6(c) illustrates three kinds of yaw damper with different nonlinear, non-smooth characteristics. Yaw damper 2 provides a small force for a small piston velocity and a large blow-off force, which results in a small linear critical speed and a supercritical bifurcation

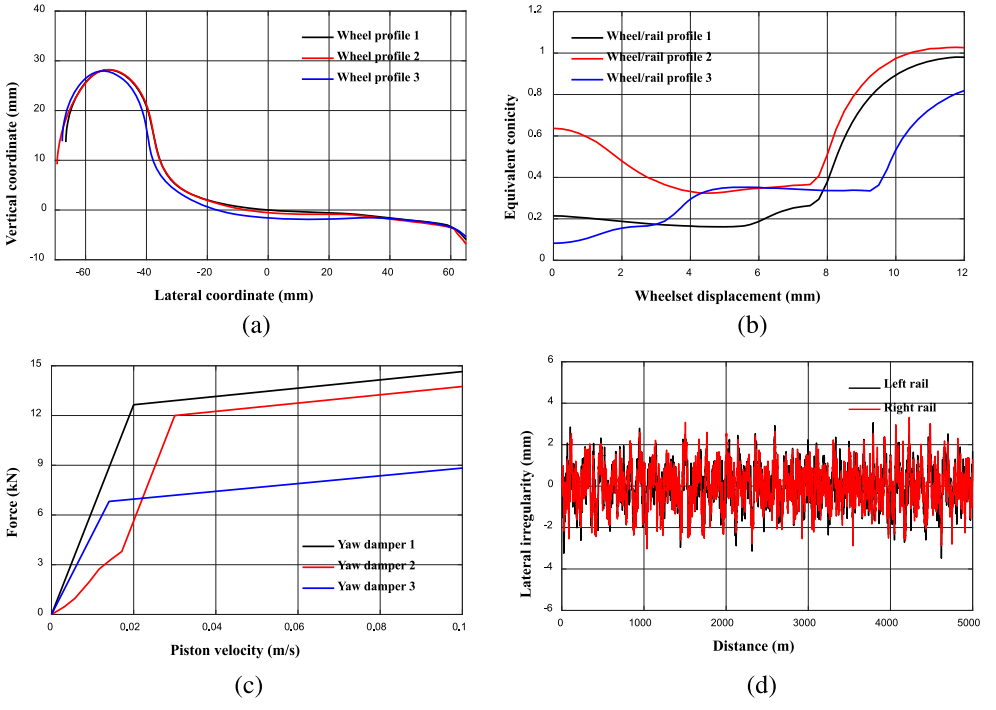


**Figure 6.** Critical parameters of the vehicle dynamic model: (a) Wheel profiles; (b) equivalent conicity; (c) nonlinear yaw damper characteristics; and (d) lateral track irregularity.

with low limit cycles. At the same time, yaw damper 3 provides a large force for a small piston velocity and a small blow-off force, which results in a large linear critical speed and a subcritical bifurcation with pronounced limit cycles [12]. Furthermore, the existing Wuhan-Guangzhou irregularity spectrum is applied in the simulation, and its lateral irregularity is illustrated in Figure 6(d).

Applying the wheel/rail contact nonlinearities and yaw damper characteristics mentioned above to the vehicle dynamic model, the bifurcation diagrams in these three cases are calculated, and the results are illustrated in Figure 7(a). The cases 1, 2 and 3 correspond to the combination of wheel/rail profile and yaw damper 1, 2 and 3, respectively. It can be observed that the vehicle in case 1 shows the supercritical bifurcation with the critical speed of 400 km/h, and the vehicle in case 2 shows the supercritical bifurcation with the critical speed of 250 km/h, and the vehicle in case 3 shows the subcritical bifurcation with the critical speed of 280 km/h. In this way, three kinds of vehicle running state can be reproduced by setting the vehicle running speed to 350 km/h: stability condition by using the parameters of case 1, SAHI conditions by using the parameters of case 2 and LAHI conditions by using the parameters of case 3.

The bogie lateral accelerations $A\_b1\_Y$ with 0.5–10 Hz band pass filtering are illustrated in Figure 7(b). It can be clearly seen that the bogie acceleration signals in both case 2 and case 3 show a strong harmonic characteristic whereas, in case 1, the signal show random vibrations. Moreover, the amplitude of lateral acceleration signals measured on the bogie frame in case 3 exceeds 8 m/s$^2$ for more than 6 times consecutively, which satisfies a typical

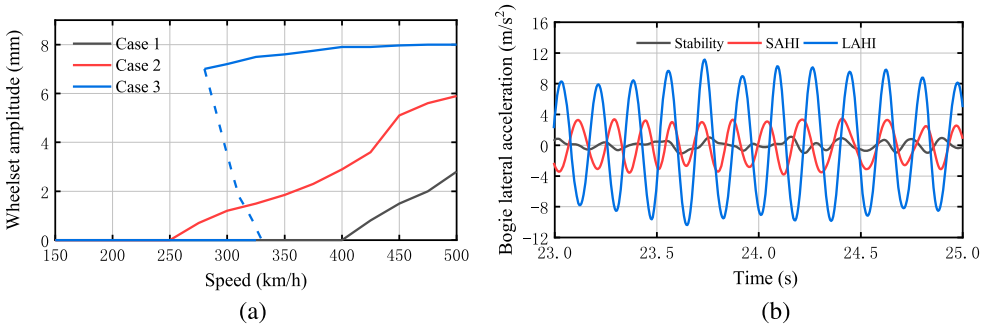


**Figure 7.** (a) Bifurcation diagram under different critical parameters and (b) bogie lateral acceleration under different vehicle states (stability, SAHI and LAHI conditions).

alarm condition [8]. The amplitude in case 2 is about 4 m/s$^2$, which is far from reaching the alarm condition and conforms to the characteristic of SAHI. Finally, the acceleration signals for cross-correlation analysis (that is all the CCIs) are collected for 30 s.

### 3.2. Selection of the most effective CCI

In this section, the proposed methodology is applied to the simulated results described in Section 3.1 to investigate the cross-correlation of the bogie frame and carbody acceleration signals in different vehicle states (stability, SAHI and LAHI conditions). Among the 8 CCIs proposed in Section 2.2 and calculated from the simulated data for all the vehicle states, the most effective indicator to identify hunting instabilities (especially SAHI) will be selected.

Considering the fluctuation of cross-correlation in the time, 21 index values have been calculated by means of sliding windows for all the CCIs (one CCI value for each second, i.e. time acquisition rate equal to 1 s). The window length has been set equal to 10 s. Figure 8 shows the CCIs in the proposed vehicle states (stability, SAHI and LAHI conditions). It can be observed that most of the CCIs almost remain unchanged near a certain mean value whereas some CCIs fluctuate a lot. For a specific CCI, a large fluctuation means a poor robustness, therefore it should be considered as an invalid indicator for hunting instability detection. Apart from the robustness, an effective CCI should show significant differences among the different vehicle running states (stability, SAHI and LAHI conditions) to effectively indicate the fault condition.

At this point, the mean values and standard deviations of each CCI for different vehicle states have been calculated and listed in Table 2. It can be seen that the standard deviations of the cross-correlation indicators *B_YY*, *C_XY*, *C_YZ* and *C_YY* are significantly larger than those of other CCIs. Furthermore, the mean values of CCIs for different vehicle states are compared in Figure 9(a) whereas the relative diagnosis indicators *D* associated to each CCI (see Equation (3)) are illustrated in Figure 9(b) for both SAHI and LAHI conditions.

An empirical interpretation of correlation coefficients CCIs is illustrated in Table 3. In general, 0.5 is regarded as the limit value for correlation analysis. When the CCI is larger than 0.5, this related signals show a significant correlation. When, on the contrary, the CCI is smaller than 0.5, this related signals show a low correlation or no correlation. The limit value is highlighted through a red dashed line in Figure 9(a). It can be observed that the

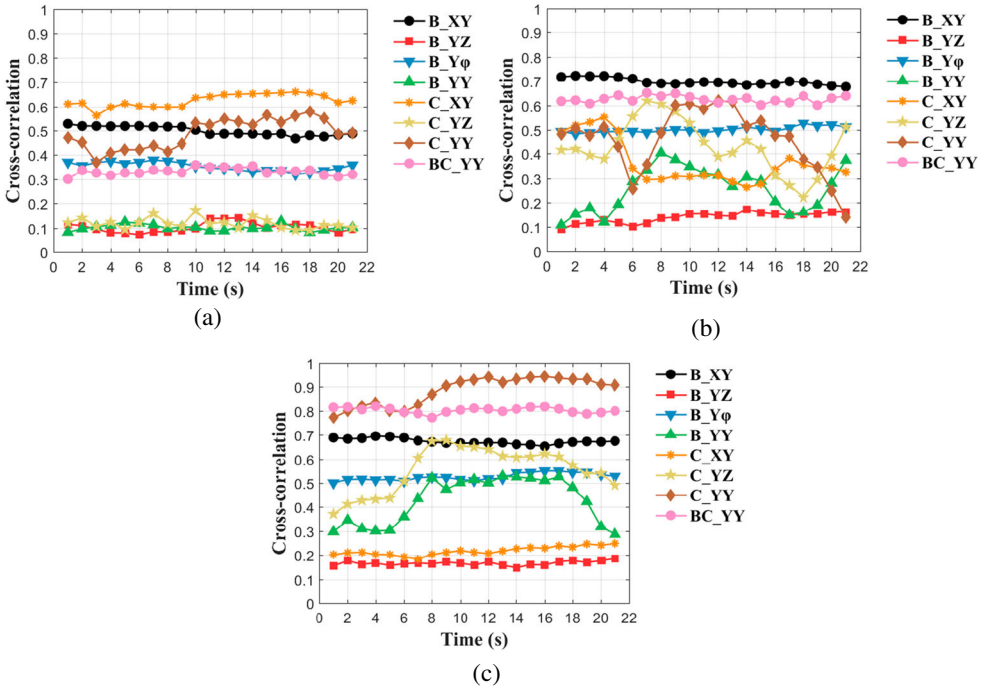


**Figure 8.** Cross-correlation indicators CCIs for different vehicle states: (a) stability; (b) SAHI; and (c) LAHI.

**Table 2.** Statistical values of CCIs for different vehicle states (stability, SAHI and LAHI).

| | Stability | | SAHI | | LAHI | |
|---|---|---|---|---|---|---|
| CCI | Mean value | Standard deviation | Mean value | Standard deviation | Mean value | Standard deviation |
| *B_XY* | 0.50 | 0.018 | 0.70 | 0.014 | 0.67 | 0.012 |
| *B_YZ* | 0.10 | 0.021 | 0.14 | 0.022 | 0.17 | 0.009 |
| *B_Yφ* | 0.35 | 0.018 | 0.50 | 0.012 | 0.53 | 0.015 |
| *B_YY* | 0.10 | 0.012 | 0.25 | 0.091 | 0.43 | 0.096 |
| *C_XY* | 0.63 | 0.027 | 0.37 | 0.092 | 0.22 | 0.018 |
| *C_YZ* | 0.12 | 0.022 | 0.43 | 0.107 | 0.56 | 0.095 |
| *C_YY* | 0.49 | 0.062 | 0.46 | 0.131 | 0.88 | 0.060 |
| *BC_YY* | 0.33 | 0.015 | 0.63 | 0.015 | 0.80 | 0.012 |

**Table 3.** Empirical interpretation of the correlation coefficients [32].

| Correlation coefficient *r* (the CCIs) | Degree of correlation |
|---|---|
| $0 \leq \lvert r \rvert < 0.30$ | Weak or no correlation |
| $0.30 \leq \lvert r \rvert < 0.50$ | Low correlation |
| $0.50 \leq \lvert r \rvert < 0.80$ | Significant correlation |
| $0.80 \leq \lvert r \rvert < 1.00$ | Strong correlation |

cross-correlation indicators *B_XY*, *B_Yφ* and *BC_YY* exceed the limit value under both the SAHI and LAHI conditions.

At the same time, the relative diagnosis indicator *D*, highlighting the volatility of CCIs, are calculated between the conditions of stability and instability (both in the SAHI and in

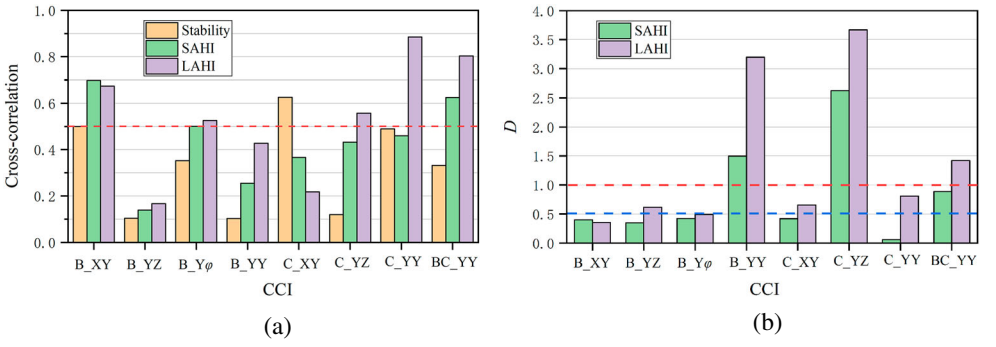


**Figure 9.** Summary of the cross-correlation analysis results: (a) mean cross-correlation indicators CCIs (for stability, SAHI and LAHI); and (b) relative diagnosis indicators (both for SAHI and LAHI).

the LAHI cases). A large value of $D$ means a good discrimination between the baseline and fault cases, and tow limit values are initially proposed for the fault diagnosis. The first limit is set equal to 0.5 (blue dashed line in Figure 9(b)) for the SAHI case whereas the second limit is set equal to 1.0 (red dashed line in Figure 9(b)) for the LAHI case. It can be observed that the relative diagnosis indicator $D$ for the cross-correlator indicators (ICCs) *B_YY*, *C_YZ* and *BC_YY* exceed the limit values under both SAHI and LAHI conditions. However, considering the small mean values and the high standard deviations of some CCIs, it would be unreasonable to evaluate the effectiveness of the CCIs only by using the relative diagnosis indicator $D$. For example, the diagnosis indicator $D$ related to *B_YY*, exceeds 1.5 under SAHI conditions and exceeds 3.0 under LAHI conditions; at the same time, the cross-correlation indicator *B_YY* is less than 0.3 under SAHI conditions and less than 0.5 under LAHI conditions. Consequently, in this case, the small mean value and the high standard deviation of the considered CCI may deeply affect the results in terms of relative diagnosis operator $D$, making the instability detection procedure quite unreliable.

Therefore, to face this problem, the following more accurate requirements are proposed to determine the most effective CCI for hunting instability detection:

- the standard deviation of cross-correlation indicators CCI for different vehicle states (stability, SAHI and LAHI conditions) should be less than 0.08;
- the mean value of cross-correlation indicators CCI for different vehicle states (SAHI and LAHI conditions) should be larger than 0.5;
- the relative diagnosis indicator $D$ for the considered CCI should be larger than 0.5 for the SAHI vehicle state and larger than 1.0 for the LAHI vehicle state.

Looking at the results of the simulation campaign described in these sections, only the cross-correlation indicator *BC_YY*, among the proposed CCIs, fully satisfies the previous requirements. The cross-correlation indicator *BC_YY* is therefore the most promising candidate for hunting instability detection and will be exploited in the following of the work.

Furthermore, to distinguish the hunting instability (especially SAHI) with the stability, the critical value of *BC_YY* should be determined. Applying the simulation models corresponding to cases 2 and 3 aforementioned, the limit cycle amplitude of wheelset and the

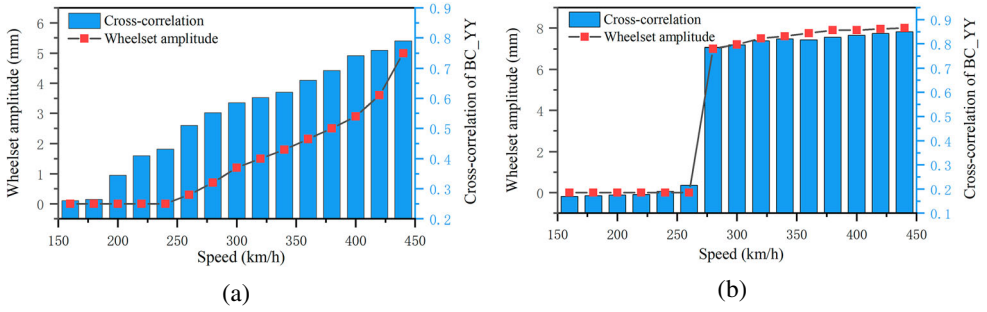


**Figure 10.** Behaviour of the wheelset amplitude and the mean cross-correlation indicator BC_YY as a function of the vehicle speed under the condition of (a) supercritical bifurcation and (b) subcritical bifurcation.

cross-correlation indicator *BC_YY* at specified vehicle speeds are calculated and plotted together in Figure 10. For the supercritical bifurcation, the *BC_YY* increases as the vehicle speed increases, and it exceeds 0.5 for the first time at the speed of 260 km/h where the vehicle starts showing a small amplitude hunting instability. For the subcritical bifurcation, the *BC_YY* doesn't exceed 0.2 when the vehicle speed is below the critical speed. Once the vehicle speed exceeds the critical speed, both the wheelset amplitude and the *BC_YY* suddenly reach a quite large value. To detect the hunting instability effectively (especially for SAHI), the critical value of *BC_YY* is set to 0.5 finally.

### 3.3. Efficiency

The computation efficiency is a key indicator for evaluating the merits of a real-time monitoring method. The comparison of the efficiency between the proposed methodology and the method adopted in Reference [21] is performed by processing the same acceleration signals duration equal to 10 s. The calculations have been performed on a quite standard Dell Inspiron 15-7559 computer with an Intel Core i7-6700HQ @2.6 GHz and a NVIDIA GeForce GTX 960M. As a result, the calculation time of the cross-correlation analysis in the proposed methodology is only 0.02 s, whereas the calculation time of the method in Reference [21] exceeds 0.3 s. Obviously, the proposed methodology has a good performance in terms of computational efficiency.

## 4. Robustness of the proposed methodology

The proposed methodology has been developed by detecting the periodic components between 0.5 and 10 Hz in the lateral acceleration signals on the bogie frame and carbody floor. However, not only the hunting instability but also the periodical excitation coming from the track can cause some effect on these signals and their cross-correlations in such frequency range. The hunting instability is a self-excited vibration while the response under periodic excitation is a forced vibration. As the origins and effects of these two abnormal vibration are different, it is important to distinguish the hunting instability from track periodic excitation during the operation.

In this robustness analysis, the new excitation due to track lateral irregularities is obtained by superimposing a harmonic excitation with wavelength equal to 20 m on the

original lateral irregularity wavelength distribution. The total amplitude distribution and the Power Spectral Density (PSD) of the combined lateral irregularities are illustrated in Figure 11(a), in which the harmonic excitation amplitude is equal to 1 mm. The frequency of the periodical excitation is 4.9 Hz at the vehicle speed of 350 km/h, which is included in the frequency range of 0.5–10 Hz considered for the lateral acceleration signals. Integrating the track lateral irregularity into the simulation model under the vehicle state of stability, the time-domain and spectra of the bogie's lateral acceleration with 0.5–10 Hz band pass filtering are obtained, as shown in Figure 11(b). It is seen that the periodic components and the dominant frequency are noticeable even if their amplitudes are relatively small. In this way, the cross-correlation analysis should be carried out further to distinguish these two cases.

Three kinds of harmonic excitation with amplitudes equal to 1, 2 and 3 mm are used to study the robustness of the methodology. The new irregularities are then integrated into the simulation model corresponding to the vehicle state of stability, SAHI and LAHI respectively. The mean cross-correlation indicators *B_YY* and *BC_YY* for the considered irregularity levels (1, 2 and 3 mm) are calculated and compared with the original cross-correlation (without periodic irregularity, namely 0 mm) for the vehicle states of stability, SAHI and LAHI, as shown in Figure 12. It can be observed that both the cross-correlation indicators *BC_YY* and *B_YY* increase with increasing excitation amplitudes under all the vehicle states. With regard to *BC_YY*, when the vehicle is under the state of stability, the cross-correlation increases only a little under the excitation amplitude equal to 1 mm whereas it exceeds 0.6 and 0.7 for the excitation amplitudes equal to 2 and 3 mm, respectively. These results conflict with the results for SAHI and LAHI conditions reported in

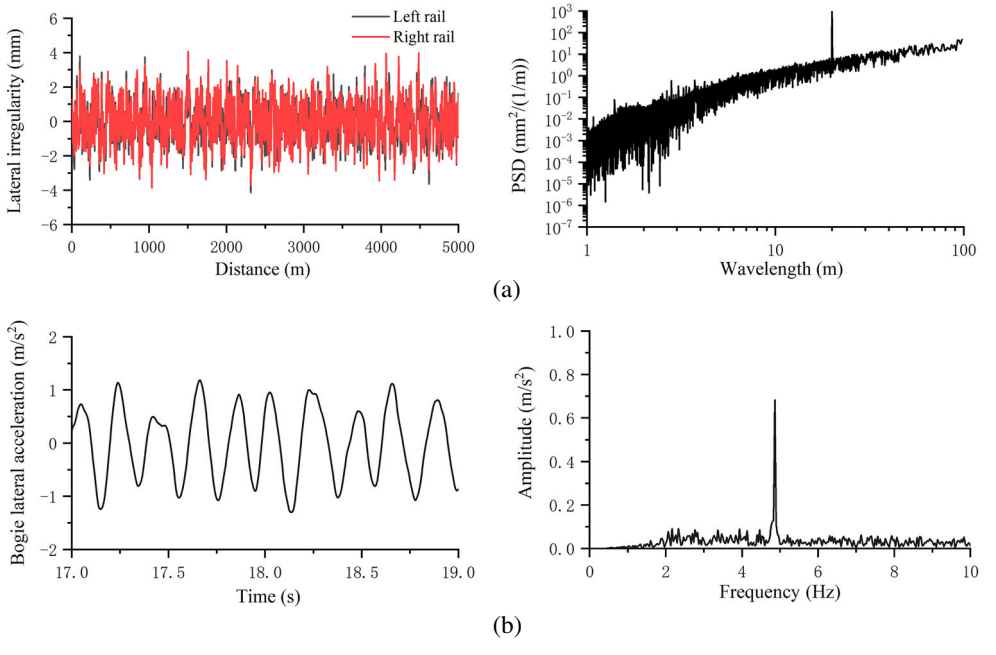


**Figure 11.** Robustness analysis: (a) amplitude distribution and PSD of the lateral irregularity; and (b) time-domain and spectra of the bogie's lateral acceleration.

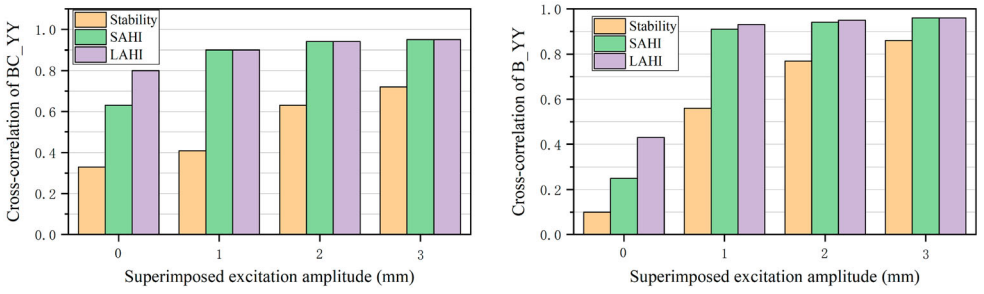


**Figure 12.** Results for the mean cross-correlation indicators *BC_YY* and *B_YY* for different irregularity levels under different vehicle states (stability, SAHI and LAHI).

Figure 8(b,c) where periodic track irregularities are not considered. In fact, in this case, it is not possible to understand if the cause of the *BC_YY* increase is the hunting instability or the track irregularity or both.

However, as regards the cross-correlation indicator *B_YY*, when the vehicle is under the state of stability, the cross-correlation increases significantly in presence of periodic track irregularities, and it reaches values near 0.8–0.9 for excitation amplitudes equal to 2 and 3 mm (see Figure 12). On the contrary, looking at the results reported in Figure 8(b,c), it is seen that the cross-correlation indicator *B_YY* is always below 0.5 in absence of periodic irregularities, both under SAHI and LAHI conditions. The main reason for that is probably that, even though the structure and characteristics of front and rear bogies are the same, the damping ratios and the hunting mode frequencies of front and rear bogies are different at the same speed [33]. Furthermore, in the actual operation of high-speed trains, the wheel profiles of the front and rear bogies may be different as well. All these reasons may lead to a smaller cross-correlation indicator *B_YY*. Furthermore, it can be observed that both the cross-correlation indicators *BC_YY* and *B_YY* exceed 0.9 in presence of periodic track irregularities, both under SAHI and LAHI conditions.

The previous considerations suggest that the cross-correlation indicator *B_YY* can be effectively used to distinguish the hunting motion from the periodic excitations due to track irregularities. More particularly, the origin of the periodic components between 0.5 and 10 Hz in the lateral acceleration signals on the bogie frame and carbody floor can be determined as follows:

- The origin is due to hunting instability, if the cross-correlation indicator *BC_YY* exceeds 0.5 and the cross-correlation indicator *B_YY* does not exceed 0.5.
- The origin is due to track irregularities, if the cross-correlation indicator *BC_YY* is between 0.5 and 0.8, whereas the cross-correlation indicator *B_YY* exceeds 0.5.
- The origin is due to both the hunting instability and the track irregularities, if the cross-correlation indicator *BC_YY* is exceeds 0.8, whereas the cross-correlation indicator *B_YY* exceeds 0.8.

## 5. Experimental validation of the methodology

The proposed methodology has been experimentally validated through a specific field test. The field test has been performed on a Chinese high-speed train running from

Guangzhou to Shenzhen. The on-boarder data acquisition system is used to continuously record the accelerations (measured through suitable accelerometers as shown for example in Figure 13). All the required acceleration signals on bogie frame and carbody were collected according to Section 2 to properly calculate the CCIs (see Section 3) and to verify the proposed instability detection methodology.

After the processing of the test data, the acceleration signals coming from the accelerometers are analysed. A 0.5–10 Hz band pass filtering is performed on the acceleration signals measured on the bogie frame and on the carbody. By way of example, both the time-domain signals and the short time Fourier transform (STFT) of the filtered acceleration signals are illustrated in Figure 14 for *A_b*1*_y* and *A_c*1*_y*. As for the peak value, the lateral acceleration of bogie frame *A_b*1*_y* is within 4 m/s$^2$, which is far from reaching the alarm limit [8]. However, the energy of vibration around 8 Hz is prominent in the time interval 260–300 s. With regard to the carbody *A_c*1*_y*, a vibration around 1 Hz is present for almost in the whole time history and is related to the rigid mode of the carbody. Furthermore, also in this case, the vibrations around 8 Hz during the period of 260–300 s is significantly larger than that in other sections.

Looking at the measurements of the accelerometers *A_b*1 and *A_c*1, SAHI probably occurs during the time interval 260–300 s. To further verify the conjecture, a local zoom of the accelerations *A_b*1*_y* and *A_c*1*_y* in the suspected time section is illustrated in Figure 15, which highlights a common harmonic vibration in the vehicle components (bogie and carbody) at a frequency of around 8 Hz.

At this point, to verify the conjecture, the cross-correlation analysis is then performed on the specific acceleration signals. Figure 16 shows the time history of cross-correlation indicators *BC_YY* and *B_YY*. It can be observed that, concerning *BC_YY*, the cross-correlation signal is below 0.5 almost everywhere, however, the cross-correlation indicator *BC_YY* corresponding to the period of 260–300 s reaches nearly 0.8 and is significantly larger than that in the other time sections. Moreover, the cross-correlation indicator *B_YY* is always below 0.5, which excludes the possibility of a periodic excitation conclusion from the track. According to the criteria reported in Sections 3 and 4, it may be inferred that the vehicle

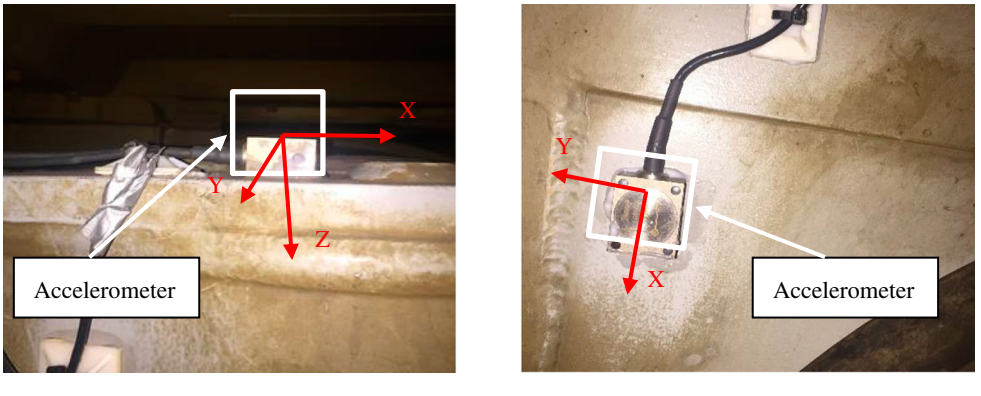


**Figure 13.** Field test campaign: (a) accelerometer *A_b*1 (see Section 2) on bogie frame above axle box and (b) accelerometer *A_c*1 (see Section 2) on the carbody floor.

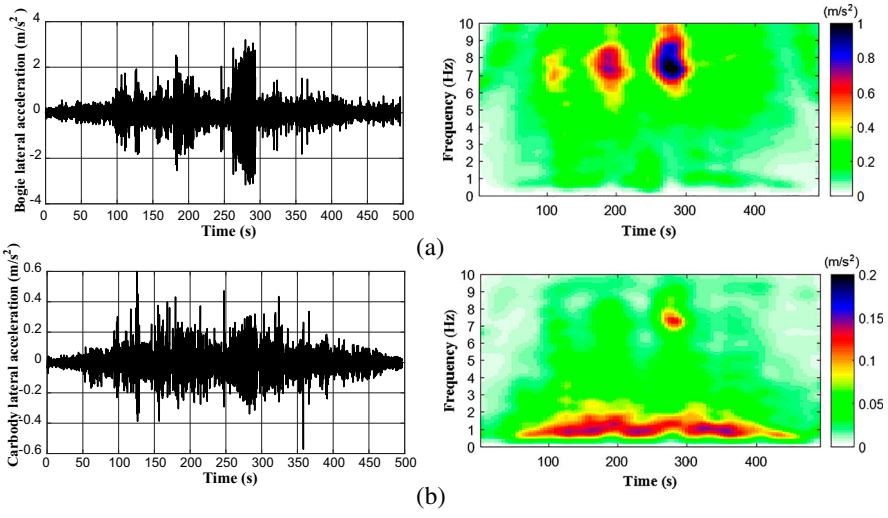


**Figure 14.** Time-domain signals and STFTs of the tested accelerations (a) *A_b*1*_y* from the bogie frame and (b) *A_c*1*_y* from the carbody.

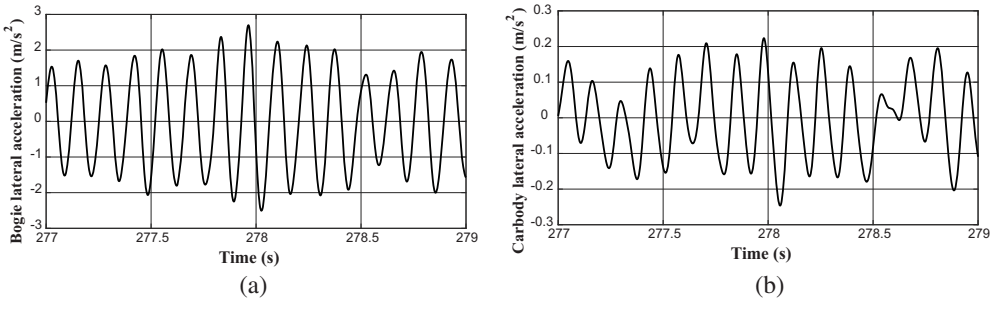


**Figure 15.** Local zoom of the lateral accelerations *A_b*1*_y* and *A_c*1*_y* in the SAHI time section.

experienced SAHI during the time interval 260–300 s, and the result further confirms the initial conjecture on the presence of SAHI based on the time-domain and STFT experimental data. Consequently, the proposed instability detection methodology turns out to be able to identify SAHI condition effectively.

Finally, to better highlight the connection between wheel/rai profile conditions (from new to worn), bogie or carbody accelerations and CCIs, and instability conditions (both SAHI and LAHI), the relation between the maximum value of bogie lateral acceleration *A_b*1*_y* and the cross-correlation indicator *BC_YY* has been investigated. More particularly, several measurements have been performed on the vehicle for different travelled distances after turning intervention and, consequently, for different wheel/rail profile conditions (from new to worn). The acceleration signals have been measured on the same part of the track and are referred to the same time window.

Figure 17 shows the variation of the maximum values of the bogie lateral acceleration *A_b*1*_y* and of the cross-correlation indicator *BC_YY* for increasing running distances of the considered high-speed railway vehicle after the turning intervention. It can be seen

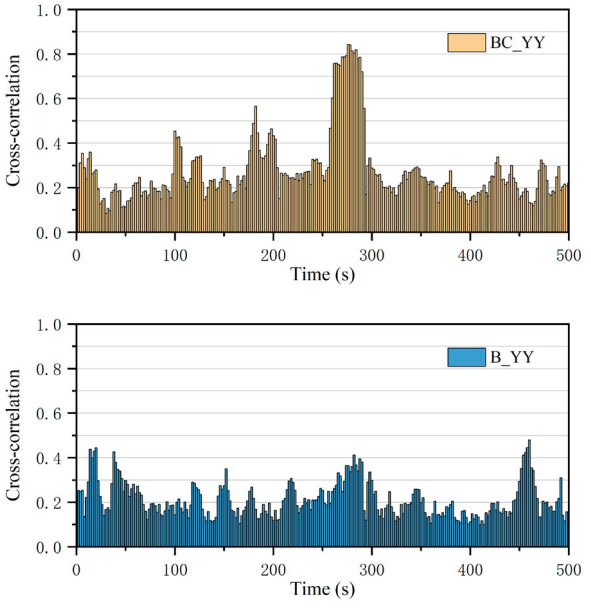


**Figure 16.** Experimental cross-correlation results of the *BC_YY* and *B_YY*.

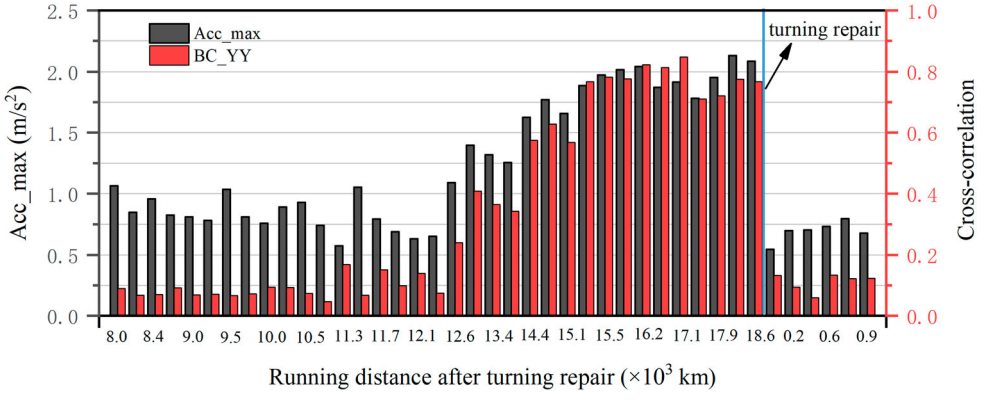


**Figure 17.** The evolution of the maximum values of the bogie lateral acceleration *A_b1_y* and the cross-correlation indicator *BC_YY*.

that, when the running distance does not exceed 12.6 × $10^3$ km, the maximum values of acceleration are all below 1.0 m/s$^2$ and only have little changes whereas the maximum of the cross-correlation indicator *BC_YY* are all below 0.2. When the running distance exceeds 12.6 × $10^3$ km, the maximum values of both acceleration and cross-correlation indicator *BC_YY* increase gradually with increasing running distance, and show a similar behaviour. When the running distance reaches 14.4 × $10^3$ km, the cross-correlation indicator *BC_YY* exceeds 0.5 whereas the maximum value of the acceleration exceeds 1.5 m/s$^2$ for the first time, a noteworthy value for this vehicle. Finally, when the running distance reaches 18.6 × $10^3$ km, the wheel profiles are repaired through a turning intervention and the new profiles are restored. The maximum value of acceleration and the

cross-correlation indicator *BC_YY* drop to a very small level immediately, and the hunting instability disappears.

The last results show again the connection between wheel/rail profile conditions, bogie or carbody accelerations and CCIs, and instability condition, and highlight very well the capability of the proposed methodology of detection hunting instability conditions (especially in the SAHI case).

## 6. Conclusions

Based on the cross-correlation analysis techniques, a new methodology for hunting instability detection (especially for small amplitude hunting instability) of high-speed railway vehicles has been proposed in this paper. The following important conclusions can be drawn:

(1) The evidence from this study suggests that there exists a strong correlation between the bogie frame and the carbody vibrations during the hunting instability. More particularly, the cross-correlation between the lateral accelerations of the bogie frame and carbody increases with the increasing of the hunting instability amplitudes, and this phenomenon can be effectively exploited to detect the small amplitude hunting instability.
(2) Combining the cross-correlation indicators BC_YY and B_YY, the proposed detection methodology can identify the origin of the vibration by distinguishing the hunting instability from the periodic track irregularities. This aspect is innovative and can be also helpful to reduce or eliminate abnormal vibrations on railway vehicle specifically.
(3) The sensor network of the proposed detection method consists of just four accelerometers mounted on the front left and rear right of the bogie fames and carbody (see Figure 4), which is compatible with most of the existing monitoring system on the high-speed railway vehicles. Furthermore, the implementation costs are quite low and the algorithm is really efficient because it is based only on simple signal processing techniques.
(4) Due to the limitation of experimental resources, this paper only considered one typical high-speed railway vehicle to validate the proposed detection methodology. Further numerical and experimental validations are required to verify the performance of the proposed methodology for different types of trains, wheel/rail profiles and bifurcation diagrams.

## Disclosure statement

No potential conflict of interest was reported by the author(s).

## Funding

This research has been supported by the Independent Subject of State Key Laboratory of Traction Power [grant number 2018TPL_T04], the National Key R&D Program Subsidized Project [grant number 2018YFB1201700], and by the National Science Foundation for Young Scholars [grant number 51805450].

## ORCID

*Jianfeng Sun* http://orcid.org/0000-0002-1551-4704
*Maoru Chi* http://orcid.org/0000-0001-6111-2768

## References

[1] Wickens AH. The dynamics of railway vehicles-from Stephenson to Carter. Proc Inst Mech Eng F J Rail Rapid Transit. 1998;212(3):209–217.
[2] Knothe K, Böhm F. History of stability of railway and road vehicles. Veh Syst Dyn. 1999;31(5-6):283–323.
[3] International Union of Railways. UIC Code 518, testing and approval of railway vehicles from the point of view of their dynamic behaviour-safety – track fatigue-ride quality. Paris: International Union of Railways; 2003.
[4] British Standards Institute. BS EN, 14363 railway applications – testing for the acceptance of running characteristics of railway vehicles – testing of running behavior and stationary tests. Valenciennes: Interoperability Unit; 2005.
[5] Official Journal of the European Union. 2008/232/EC Concerning a technical specification for interoperability relating to 'rolling stock' sub-system of the trans-European high-speed rail system; 2008. Available from: http://www.ojec.com/?aspxerrorpath = /contactus.aspx
[6] Federal Railroad Administration. Vehicle/track interaction safety standards. High-speed and high cant deficiency operations. College Park: National Archives and Records Administration; 2013.
[7] CNR Sifang Rolling Stock Research Institute. TB/T3188-2007 technical specification for railway car safety monitor and diagnosis system. Beijing: China Railway Publishing House; 2008.
[8] Ministry of Railways of the People's Republic of China. TB10761-2013 high-speed railway engineering dynamic acceptance technical criterion. Beijing: Ministry of Railways of the People's Republic of China; 2013.
[9] Chen JZ. Study on theory of onboard measurement of wheel and rail forces. Chengdu: Southwest Jiaotong University; 1994.
[10] Polach O. Comparability of the non-linear and linearized stability assessment during railway vehicle design. Veh Syst Dyn. 2006;44(sup1):129–138.
[11] Polach O. Characteristic parameters of nonlinear wheel/rail contact geometry. Veh Syst Dyn. 2010;48(Suppl):19–36.
[12] Polach O. Application of nonlinear stability analysis in railway vehicle industry. In: Thomsen PG, True H, editors. Non-smooth problems in vehicle systems dynamics. Berlin: Springer; 2009. p. 15–27.
[13] Wang XR, Qu JJ, Zeng YQ. Applying vibration energy method to analyze stability against hunting of 25 t axle load low dynamic action bogie. Railw Locomot Car. 2002;6:1–5.
[14] Yao JW, Sun LX, Hou FG. Study on evaluation methods for lateral stability of high-speed trains. China Railw Sci. 2012;33(6):132–139.
[15] Gasparetto L, Alfi S, Bruni S. Data-driven condition-based monitoring of high-speed railway bogies. Int J Rail Transp. 2013;1(1):42–56.
[16] Ning J, Cui WL, Chong CJ, et al. Feature recognition of small amplitude hunting signals based on the MPE-LTSA in high-speed trains. Measurement (Mahwah N J). 2019;131:452–460.
[17] Huang NE, Shen Z, Long SR. The empirical mode decomposition and the Hilbert spectrum for nonlinear and non-stationary time series analysis. Proc R Soc Med. 1998;454:903–995.
[18] Ye YG, Ning J, Chong CJ, et al. Hunting instability of high-speed train diagnose method based on modified ensemble empirical mode decomposition Shannon entropy and LSSVM. Appl Res Comput. 2017;34(04):1097–1100.
[19] Liu Q, Ning J, Ye YG, et al. Study on hunting instability of high-speed train based on EEMD and energy entropy. China Meas Test. 2017;43(05):96–100.

[20] Ye YG, Ning J. Small-amplitude hunting diagnosis method for high-speed trains base on the bogie frame's lateral-longitudinal-vertical data fusion, independent mode function reconstruction and linear local tangent space alignment. Proc Inst Mech Eng F J Rail Rapid Transit. 2019;233(10):1050–1067.
[21] Song XW. Research for hunting instability detection of bogie by lateral motion identification method. Chengdu: Southwest Jiaotong University; 2017.
[22] Wei L, Zeng J, Chi MR, et al. Carbody elastic vibrations of high-speed vehicles caused by bogie hunting instability. Veh Syst Dyn. 2017;55(9):1321–1342.
[23] Mei TX, Ding XJ. A model-less technique for the fault detection of rail vehicle suspensions. Veh Syst Dyn. 2008;46(S1):277–287.
[24] Mei TX, Ding XJ. Condition monitoring of rail vehicle suspensions based on changes in system dynamic interactions. Veh Syst Dyn. 2009;47(9):1167–1181.
[25] Li CS, Luo SH, Cole C, et al. Bolster spring fault detection strategy for heavy haul wagons. Veh Syst Dyn. 2018;56(10):1604–1621.
[26] Li CS, Luo SH, Cole C, et al. A signal-based fault detection and classification method for heavy haul wagons. Veh Syst Dyn. 2017;55(12):1807–1822.
[27] Haugh LD. Checking the independence of two covariance stationary time series: a univariate residual cross-correlation approach. J Amer Statist Assoc. 1976;71:378–385.
[28] Rajamani P, Dey D, Chakravorti S. Cross-correlation-aided fuzzy c-means for classification of dynamic faults in transformer winding during impulse testing. Electr Power Compon Syst. 2010;38(13):1513–1530.
[29] Chandaka S, Chatterjee A, Munshi S. Cross-correlation aided support vector machine classifier for classification of EEG signals. Expert Syst Appl. 2009;36:1329–1336.
[30] UIC Code 519. Method for determining the equivalent conicity. 1st ed. Paris: International Union of Railways; 2004.
[31] Polach O. On non-linear methods of bogie stability assessment using computer simulations. Proc Inst Mech Eng F J Rail Rapid Transit. 2006;220(1):13–27.
[32] Yuan Z. Quantitative analysis of public administration: methods and techniques. Chongqing: Chongqing University Press; 2006.
[33] Matsudaira T. Hunting problem of high-speed railway vehicles with special reference to bogie design for the new Tokaido line. Proc Inst Mech Eng F J Rail Rapid Transit. 1965;180(6):58–66.

# Appendix

**Table A1.** Primary parameters of the railway vehicle.

| Notation | Parameter | Value | Unit |
|---|---|---|---|
| $M_c$ | Car body mass | 40,384 | kg |
| $M_t$ | Bogie frame mass | 2800 | kg |
| $M_w$ | Wheelset mass | 1713 | kg |
| $I_{cx}$ | Roll moment of inertia of car body | 93,303 | kg·m$^2$ |
| $I_{cz}$ | Yaw moment of inertia of car body | 1,552,360 | kg·m$^2$ |
| $I_{tx}$ | Roll moment of inertia of bogie frame | 1846 | kg·m$^2$ |
| $I_{tz}$ | Yaw moment of inertia of bogie frame | 2792 | kg·m$^2$ |
| $I_{wz}$ | Yaw moment of inertia of wheelset | 1050 | kg·m$^2$ |
| $K_{px}$ | Longitudinal locating stiffness of axle-box | 85 | MN/m |
| $K_{py}$ | Lateral locating stiffness of axle-box | 5 | MN/m |
| $K_{pz}$ | Vertical stiffness of primary suspension | 0.95 | MN/m |
| $K_{sx}$ | Longitudinal stiffness of secondary suspension | 0.15 | MN/m |
| $K_{sy}$ | Lateral stiffness of secondary suspension | 0.15 | MN/m |
| $K_{sz}$ | Vertical stiffness of second suspension | 0.21 | MN/m |
| $C_{py}$ | Lateral damping of primary suspension | 10 | kN·s/m |
| $C_{pz}$ | Vertical damping of primary suspension | 10 | kN·s/m |
| $C_{sy}$ | Lateral damping of secondary suspension | 20 | kN·s/m |
| $C_{sz}$ | Vertical damping of secondary suspension | 10 | kN·s/m |
| $K_d$ | dynamic stiffness of yaw damper | 5 | MN/m |
| $C_d$ | dynamic damping of yaw damper | - | kN·s/m |